Published in final edited form as:
Electrophoresis. 2014 May ; 35(9): 1214–1225. doi:10.1002/elps.201300451.

Recent advances in coupling capillary electrophoresis based separation techniques to ESI and MALDI MS

Xuefei Zhong[1,†], **Zichuan Zhang**[1,†], **Shan Jiang**[1], and **Lingjun Li**[1,2,*]

[1]School of Pharmacy, University of Wisconsin, 777 Highland Avenue, Madison, Wisconsin 53705, United States

[2]Department of Chemistry, University of Wisconsin, 1101 University Avenue, Madison, Wisconsin 53706, United States

Abstract

Coupling capillary electrophoresis (CE) based separation techniques to mass spectrometry creates a powerful platform for analysis of a wide range of biomolecules from complex samples because it combines the high separation efficiency of CE and the sensitivity and selectivity of MS detection. ESI and MALDI, as the most common soft ionization techniques employed for CE and MS coupling, offer distinct advantages for biomolecular characterization. This review is focused primarily on technological advances in combining CE and chip-based CE with ESI and MALDI MS detection in the past five years. Selected applications in the analyses of metabolites, peptides, and proteins with the recently developed CE-MS platforms are also highlighted.

Keywords

CE; ESI; interface; MS detection; MALDI

1 Introduction

Featuring minimum sample and solvent consumption, rapid separation speed, high resolving power, capillary electrophoresis (CE) finds extensive applications in the area of metabolomics [1, 2], bottom-up proteomics [3–7], as well as glycan [8] and intact protein analyses [9] when it is interfaced with versatile modes of mass spectrometry (MS) detection. A variety of soft ionization techniques have been employed for both on-line and off-line coupling of CE and MS, such as electrospray ionization (ESI), atmospheric pressure chemical ionization, atmospheric pressure photoionization, matrix-assisted laser desorption/ionization (MALDI) [10]. Among these ionization methods, ESI is the most popular approach for on-line CE-MS coupling due to the ease of implementation and the compatibility with a large category of molecules, from small metabolites to intact proteins. Off-line coupling of CE and MS by MALDI also attracts lots of interests because of higher tolerance with salts, better sensitivity of specific category of analytes, and the versatility of separation modes and buffer choice. As ESI and MALDI are the most prevalent ionization

[*]**Corresponding author**. Tel.: (608) 265-8491, Fax: (608) 262-5345, lli@pharmacy.wisc.edu.
[†]These authors contributed equally to this work.

methods employed for biomolecule analysis and they offer distinct advantages in different applications, in this review, we focus discussion on the technical developments of CE-MS coupling with these two ionization methods in recent five years.

2 On-line coupling of CE and ESI-MS

Although CE and ESI share some common properties, such as they both employ simple direct current circuits, and are both amenable to analysis of biomolecules, strategies for successful application of CE- ESI-MS must address several fundamental issues, including i) consolidation of the CE and ESI circuits; ii) stable electric contact at the CE outlet electrode; iii) proper emitter geometry for supporting stable electrospray ionization; iv) suitable electrolyte for separation and electrospray ionization. As scientists working in this area are pursuing better sensitivity, physical robustness, reproducibility and stability, several improved CE-ESI-MS interfacing strategies emerged in recent years. Fundamentals and details of CE-ESI-MS interface designs were discussed in several previously published reviews [10–14]. The following discussions will be focused on recent technological improvements of these CE-ESI-MS coupling strategies.

2.1 CE-ESI-MS interfaces employing sheath-flow or make-up flow liquid

The most common and commercially available sheath liquid interface uses a coaxial arrangement for three concentric tubing: the separation column, the straight metal tubing for sheath liquid delivery and the outer tubing for nebulizer gas [15]. The sheath liquid metal tubing functions as the CE outlet electrode and the electrospray emitter. The sheath liquid serves to establish electric contact between the metal tubing and the background electrolyte in the separation column, and to modify the components of the background electrolyte for improved ionization efficiency. The separation column usually extrudes out of the sheath liquid tubing by 1~2 millimeters to avoid any dead volume and produce stable spray. As the dimension of the sheath liquid metal tubing must be large enough to accommodate the most frequently used silica capillary columns (360 μm OD), relatively larger flow rate of sheath liquid (usually 1~10 μL/min) is required to maintain stable electrospray ionization and a nebulising gas could be used to accelerate solvent evaporation in the ion source. This interface design has been adopted by many researchers for years due to its robustness, ease of assembling, versatile choice of background electrolyte (BGE) solution, and almost zero dead volume. However, two major weaknesses of this interface cannot be ignored. Firstly, the high-flow rate sheath liquid introduces significant dilution effect for the CE effluent. Secondly, nebulising gas causes a suction effect at the capillary outlet and induces parabolic flow inside the capillary, which decreases the separation efficiency. Although this suction effect could be corrected by applying a negative pressure at the CE inlet vial, extra efforts are needed to determine the precise pressure to be applied at the inlet. Reducing the flow rate of sheath liquid becomes a key factor for improving the overall sensitivity of this type of interface and avoiding the use of a nebulising gas. Efforts towards going down to nanospray region have been made by several groups.

The Sweedler group used a scaled-down version of the conventional sheath liquid interface to achieve improved sensitivity [16–18]. In order to work in the sub-microliter per minute sheath liquid flow rate region, they reduced the OD and ID of the stainless steel (s.s) sheath

liquid tubing to 260 μm and 130 μm respectively [17]. Accordingly, the separation column that goes through the s.s. tubing was also scaled down to 110 μm ID and 40 μm ID [17]. The separation capillary column end protruded 20−200 μm beyond the metal capillary tube for optimized spray [18]. In this configuration, sheath liquid infused at 0.75 to 1 μL/min by syringe pump was enough to support a stable Taylor cone for electrospray and nebulizer gas could be eliminated. With the reduced sheath liquid flow rate, this CE-ESI-MS interface provided enough sensitivity to investigate metabolites and neurotransmitters from single neurons on a Bruker MaXis Q-ToF platform [16–20].

The liquid junction interface is another type of CE-ESI-MS interface that employs make-up flow liquid at the capillary terminus. The make-up flow liquid is usually added to the CE effluent via a 20 – 200 μm gap between the capillary end and the spray emitter. A pressurized nanospray interface which used fused silica as nanospray emitters showed improved performance in a series of applications [21–25]. Some parameters, such as the width of the gap between the capillary end and the emitter, counter-balanced pressures at the capillary inlet and the liquid junction, were demonstrated to be important for good separation efficiency [26].

Both Chen group [27] and Dovichi group [28] adopted the ‘junction-at-the-tip’ concept for the low-flow sheath liquid CE-ESI-MS interfaces. With this arrangement, the end of the CE separation column reaches as far as possible into a tapered outer tube that serves as the electrospray emitter. The separation column cannot protrude out of the emitter tip due to the gradual shrinking OD and ID of the tapered emitter tip, creating a liquid junction at the interior of the emitter tip where the sheath-liquid or make-up flow mixes with the CE effluent. The geometry of the emitter tip is the most critical factor that determines the optimal flow rate region for stable electrospray. Different solutions were implemented by the two groups to achieve a minimum sheath liquid flow rate.

By evaluating the performance of a series of s.s. electrospray emitters with different tip sizes and shapes (Figure 1A), Chen and coworkers found that with similar tip size, asymmetrical emitter geometry can accommodate a wider flow rate range and offer better sensitivity compared to the blunt tapered symmetrical shape (Figure 1B) [29]. The emitter tip geometry with 35 degree beveled tip surface and 16 degree taper angle was chosen for their later interface configuration of CE-ESI-MS, which could accommodate a typical sheath liquid flow rate range of 100−500 nL/min. The shaft of the s.s. sprayer tube has a OD 720 μm of and ID of 412 μm, making it well suited for a conventionally used 360 μm OD fused silica capillary column. Compared with a commercial sheath-flow CE-MS interface, fivefold on average improvement of limit of detection of 18 amino acids was achieved by employing a relatively low sheath liquid flow [27].

While the s.s. emitter offers better mechanical strengths, Dovichi group employed borosilicate glass capillary to fabricate electrospray emitters with tip ID of 2~10 μm by micropipette puller [28]. In spite of higher risk of tip damage and blockage, such small tip can operate in the nanospray regime and give substantially increased signal-to-noise ratio, and it only needs a minimal amount of sheath liquid flow without mechanical pumping. As electrospray voltage could not be applied directly on the glass capillary emitter, high voltage

was applied at the sheath liquid reservoir, which was connected to the spray emitter via another fused silica capillary and a PEEK cross union. By coupling this interface with an AB Sciex QTrap 5500 triple-quadrupole mass spectrometer, Li et al. demonstrated that the mass sensitivity of CE-ESI-multiple reaction monitoring (MRM) for absolute quantification of Leu-enkephalin in a complex mixture was improved by 10−20 fold compared to their previous study using nanoLC coupled with MRM [30]. This CE-ESI-MRM method was further extended to detect three abundant proteins from 100 pg of cell lysate digest, which approximates protein content from a single cell [31]. The potential application of CE-ESI-MS in bottom-up proteomics was also investigated by interfacing this nanospray sheath-flow interface to an LTQ-Orbitrap Velo mass spectrometer, whose fast scan speed is more compatible with the short separation window of CE [32–37]. Suffering from small loading capacity, CE-ESI-MS/MS is more suitable for analyzing proteome samples of intermediate complexity, such as protein secretome prefractionated with HPLC [32]. It was also demonstrated that, CE-ESI-MS/MS favors detecting peptides with higher pI and lower hydrophobicity values compared to nanoLC-MS [32]. When the peptide sample loading amount goes below 10 ng, the number of unique peptides identified by a single CE-ESI-MS/MS run exceeds that identified by a single nanoLC-ESI-MS/MS run [37].

Another common concern associated with this type of ‘junction-at-the-tip’ configuration is the post-column band broadening caused by the dead volume formed at the interior of the tapered emitter tip. Both groups conducted computational simulation and experiments to evaluate this potential problem with their interfaces. Again, geometric dimension plays an important role in the band broadening effects. For the interface developed by the Chen group, the distance from separation column end to the emitter tip outlet was around 600 μm, making a total volume of the flow-through microvial close to 20 nL [38]. The simulated flow profile and mass transport process inside the tiny flow-through microvial showed that with proper sheath liquid flow rate, peak distortion and post-column band broadening can be minimized. These results were further confirmed by comparing the UV detected peaks and MS detected peaks under similar experimental conditions [38]. For the nanospray sheath-flow interface developed by the Dovichi group, the tapered length of the glass emitter was about 3 mm, and the optimized spacing between the separation column end and the emitter tip was 1 mm [28]. The use of a 150 μm OD separation column rather than a 360 μm one reduced the dead volume enclosed by the emitter tip and the separation column end, as the 150 μm OD separation column could be inserted further into the tapered glass capillary emitter. It was demonstrated that a 2 mm gap between the separation column end and the emitter tip causes significantly broader and lower amplitude peaks compared to the 1 mm gap.

Despite the concerns discussed above, the ‘junction-at-the-tip’ design forms a flow-through microvial at the CE outlet, which creates possibilities to perform CE separation in some special modes. One example demonstrated by Maxwell et al. [39] and Jayo et al. [40] is the separation of negatively charged carbohydrates with reversed polarity and electroosmotic flow (EOF) towards the inlet. The make-up flow solution in the flow-through microvial can back-fill the capillary to maintain a continuous EOF while providing a stable forward flow at the emitter tip surface to support electrospray. This flow-through microvial also enables interfacing on-line capillary isoelectric focusing (CIEF) with ESI-MS detection [41], since

the microvial at the cathode end can supply basic catholyte solution during focusing stage and provide acidic mobilizer solution during the mobilization stage.

2.2 Sheathless interfaces for CE-ESI-MS

The sheathless CE-ESI-MS interfaces usually generates greater sensitivity since the analytes exiting the separation column does not suffer from dilution and the nanospray emitter gives fairly high ionization efficiency. However, eliminating sheath-flow liquid also restricts the choice of BGE, as BGE itself is used for nanospray without any further modification. In the absence of sheath-flow liquid, the most challenging problem is to establish stable and long-lasting electrical contact at the column outlet for completing the CE circuit and applying ESI voltage. Two categories of designs are involved in the sheathless CE-ESI-MS interfaces: the one-piece interfaces which shape the separation column ends into nanospray emitters, and the two-pieces interfaces which employ replaceable nanospray emitters.

Among various strategies of creating electric contact employed in the one-piece CE-ESI-MS interface designs, such as applying metal coating on the emitter tip, or inserting an electrode into the column end [11, 12], the porous sprayer tip [42], originally developed by Moini et al. and later licensed by Beckman Coulter, has been widely practiced in the last few years. As shown in Figure 2, the electrical connection of this interface is achieved by inserting the porous capillary outlet into a metal sheath and filling metal sheath with background electrolyte [42, 43]. This porous sprayer tip, made from etching a segment of the capillary outlet by hydrofluoric solution, allows transporting of small ions across the porous wall [44] and accommodates flow rate as low as several nanoliter per minute [45, 46]. Compatibility with such ultra-low flow rate facilitates CE-MS applications using neutral coated capillaries that exhibit only an extremely low EOF, which greatly extends the use of this sheathless CE-ESI-MS interface in solving challenging separation problems such as glycoform profiling of glycopeptides [47] and intact biopharmaceutical proteins [48]. Evaluations of the system repeatability and sensitivity of this sheathless porous tip interface were conducted by several groups using various analytes. In general, the system repeatability (RSD of migration time and peak area) was considered to be suitable for quantitative analysis of small molecules [49–51], peptides [52] and intact proteins [53]. Compared to the conventional sheath-flow liquid interface, Ramautar et al. showed that the detection limits for 20 metabolite standards were decreased by 10−30 fold, leading to two fold increase of the coverage of human urine metabolome [51]; Haselberg et al. also found 50−140 fold improvement of detection limits for four intact protein standards [53]. With this sensitivity and repeatability, CE-ESI-MS based on the sheathless porous tip interface has been used to solve a wide range of analytical problems, including study of protein-protein and protein-metal complexes under physiological conditions [54, 55], characterization of protein-drug conjugates [56], determination of amino acid racemization rates in ancient silk [57], forensic analysis of phosphorus-containing amino acid-type herbicides [58], metabolomic profiling of urine and cerebrospinal fluid samples [50, 51, 59], bottom-up proteomics [43, 60], and protein post-translation modifications [46–48, 61]. In order to improve the sample loading capacity, transient isotachophoresis (t-ITP) [45, 46, 51], and solid phase microextraction (SPME) combined with t-ITP [60] were integrated online with this sheathless interface in the applications of metabolomics and bottom-up proteomics studies. In comparison with

reversed phase nanoLC-ESI-MS, it has been shown that, CE-ESI-MS is an important platform for bottom-up proteomics studies [43, 60], and especially for phosphoproteomics [46, 61]. Heemskerk et al. developed a t-ITP-CE-ESI-MS strategy that gave superior mass sensitivity and concentration sensitivity for phosphopeptide detection [46]. They also showed that this optimized CE-MS strategy has a better chance to identify multiphosphorylated peptides, which could not be detected by the nano-LC-MS even with a higher sample loading amount [46]. The most recent research on characterization of post-translationally modified histones [61], published by Sarg et al., also demonstrated that more modified peptides and more modification sites, mainly acetylation, phosphorylation, deamidation, were found by the ultra-low flow sheathless CE-ESI-MS with 2 orders of magnitude smaller sample loading amount compared to nanoLC-MS. Figure 3 shows a detailed comparison of the number of unmodified and modified histone H1 peptides identified by CE-ESI-MS and LC-ESI-MS/MS analysis.

Efforts on improving the two-piece sheathless interface designs have also been noted. In contrast to the one-piece design, the disposable emitter made from bare-fused silica capillary can be easily replaced if clogged or damaged, and it is relatively simple to coat the capillary inner surface for specific applications. The challenges of building robust two-piece sheathless interfaces lie in aligning the separation column end and emitter with minimum gap, and maintaining stable electric contact at the joint of the two pieces. In the design made by Park et al. [62, 63], two ports of a three-port plastic tee were used to secure the separation column and the emitter, and the third one was packed with Nafion, which formed a conductive polymer layer that allows cations to move through. A piece of sponge soaked with electrolyte was placed on top of the Nafion layer and voltage for electrospray was applied through a platinum wire wrapping around the tee. In another design constructed by Her et al. recently [64], a 1 mm long, 50 μm ID microchannel made inside a polydimethylsiloxane (PDMS) microdevice was employed to connect the separation column, the capillary emitter, and the microreservoir containing BGE where ESI voltage was applied. Although dead volume at the junction of the two capillaries still existed in both designs, the authors found that the separation efficiency was not significantly affected by the gap.

2.3 Chip based CE-ESI-MS

Interfacing commercially available CE instrument to ESI-MS usually requires a capillary column length above 65 cm due to the physical distance from the CE inlet electrode to the ion source, which might cause relatively longer separation time as the maximum voltage could be applied across the column is 30 kV. Performing CE on microfabricated devices can overcome this problem because the miniaturized chip can be incorporated into the ion source and the separation channels can be customized to the desired lengths for specific applications. To spray the effluent from CE channel, either an external emitter is attached to the end of the micro-separation channel or an edge or a corner of the microdevice is shaped into a nanospray emitter. The Her group tried different methods of attaching external emitters to poly (methyl methacrylate) based CE chips. They first made a sheathless interface by fixing the back end of a conductive rubber coated capillary emitter to the outlet of the CE microchannel using epoxy resin [65], and later constructed a liquid junction

interface by connecting the microchannel and the fused-silica capillary emitter with a 1.5 cm capillary and immersing this connecting capillary in a sheath liquid reservoir [66]. Integrated nanospray emitters on glass microchips were fabricated in different approaches. Belder et al. recently described a method to modify the channel outlet of an electrophoresis glass chip into a sheathless nanospray emitter. A 300 μm diameter cone machined concentrically around the channel opening on the glass edge was drawn into a sharp tip and then etched by hydrofluoric acid [67–69]. With the tip opening around 10 μm, the integrated glass chip emitter demonstrated performance similar to that achieved by commercial nanosprayer [68]. Rather than modifying a planar edge of the glass chip into a nanospray emitter, Ramsey group used the 90 degree rectangular corner of a 300 μm thick glass chip as the electrospray emitter [70]. The CE separation channel ended at the rectangular corner, where it met the end of electroosmotic pump channel that delivers a make-up flow. A positively charged surface coating was used to eliminate adsorption of protein/peptides on the separation channel and to generate anodic electroosmotic flow. High separation efficiency achieved in several minutes using this chip-CE-ESI-MS device was demonstrated in the analysis of protein digests [70] and single cell lysate [71].

Two-dimensional separation platforms are desired in comprehensive analysis of complex biological samples because they provide improved peak capacity and resolving power. As an orthogonal separation mode to RPLC, on-chip CE is an ideal choice for the second separation dimension since its fast separation speed improves the sampling rate of the first dimension. Monolithic integration of 2D LC-CE-ESI on a glass microfluidic device [72] and coupling capillary UPLC with on-chip CE-ESI [73] (Figure 4) were recently reported by the Ramsey group. In both systems, effluent from RPLC was transferred to the CE separation channel by electrokinetically gated injections. With the large field strength (~1.1 kV/cm) for CE separation, the migration time scale for the second dimension was within only 22 seconds so that CE injections spaced 10 s apart could be used to sample peaks from the first dimension [72, 73]. At this stage, only full scan MS mode could be used to record chip-CE-ESI-MS data due to the extremely narrow CE peaks. To fully exploit the advantages of microfluidic devices for complex sample analysis, data sampling rates of mass spectrometers still need to be improved to acquire enough tandem MS spectra for structural elucidation and analyte identification [69].

3 Off-line coupling of CE and MALDI-MS

Coupling of CE with MALDI-MS detection provides an attractive alternative to CE-ESI-MS because it offers more choices for the BGE and allows for easier implementation of other separation modes besides zone electrophoresis. Most notably, MALDI-MS has better tolerance with salts compared to ESI-MS and the MALDI MS detection can be decoupled from CE separation, thus enabling independent optimization of CE separation and MS detection. Despite several reports on on-line coupling of CE and MALDI-MS [10], off-line coupling of CE with MALDI-MS detection is still more prevalent in the recent years since it does not require any modification of the MALDI source. Another advantage of off-line coupling is the number of spectra that could be acquired on the same sample spot is not limited by the data acquisition rate of the mass spectrometer or the migration time window of a transient peak. In this way, masses of interest from full MS scan can be selected for

MS/MS identification. The most critical issue for off-line CE-MALDI-MS coupling is to maintain the electric continuity while collecting the CE effluent at the capillary outlet. As both ESI-MS and MALDI-MS are post-column detection methods, some capillary outlet configurations used in CE-ESI-MS can be adapted for CE-MALDI-MS coupling, such as the coaxial sheath-flow liquid interfaces, the sheathless interfaces using metal coated capillary end, and the pressurized liquid junction interfaces. Another challenge for CE-MALDI-MS coupling is to collect the CE effluent with minimum loss of sensitivity, minimum perturbation to the separation process and maximum preserving of on-column resolution. Some commercially available MALDI spotters designed for nanoLC system can be used to collect discrete CE fractions directly on the MALDI target with precise control of the time interval for spotting and the volume of each fraction. Although the automated MALDI spotters can spot as fast as four seconds per fraction, separation resolution is still compromised and they have to be used with a sheath liquid flow. Recent development of CE-MALDI- mass spectrometry imaging (MSI) provides a viable solution to this problem. In addition, strategy of applying matrix is also crucial for generating homogeneous crystals and obtaining reproducible results. In this section, more effective off-line CE-MALDI-MS interfacing strategies and recent developments in combining different CE separation modes with MALDI-MS detection will be discussed and highlighted.

3.1 CE-MALDI-MS interfaces employing sheath-flow liquid

The sheath liquid employed in the CE-MALDI-MS interface mainly serves two purposes: 1) to keep the integrity of CE circuit by grounding the sheath liquid reservoir or the coaxial metal sheath tubing that delivers the sheath liquid; 2) to create droplet on the capillary end for easier sample deposition. The composition of sheath liquid solution can be the same as CE running buffer or even matrix for MALDI detection as long as it does not affect the separation efficiency [74]. Helmja et al attempted to develop a universal CE fraction collector apparatus for different types of subsequent mass spectrometric detection using classical coaxial sheath-flow liquid interface configuration [75]. Gravity induced sheath liquid flow (~ 2.5 μL/s) formed droplets at the capillary tip, which can be detected by a light emitting diode droplet counter when falling from the capillary tip. The volume of each droplet largely depends on the capillary outer diameter. In this report, 12~18.5 μL per fraction/droplet, relatively large compared to the nanoliter volume of a CE peak, was collected in PCR tubes located on a moving x/y stage. Rather than continuously delivering sheath liquid, a ‘drop on demand’ sheath liquid CE-MALDI interface, employing a high-speed inkjet printer valve to dispense matrix sheath liquid to the capillary end in pulses, was developed by Vannatta and co-workers [76]. The distal end of CE separation capillary was inserted into a 190 μm ID nozzle through a tee, and the matrix flow was applied through another port of the tee and controlled by a dispensing valve. A CE fraction was deposited onto the MALDI plate fixed to a microscope x/y stage every 750 milliseconds. With this fast deposition rate, separation efficiency with up to 40 000 theoretical plates was achieved in less than 3 minute separation, and over 70% of sequence coverage was obtained for tryptic digested α-lactalbumin in the subsequent MALDI-ToF detection.

3.2 Sheathless interfaces for CE-MALDI-MS

Although sheathless interfaces can provide better sensitivity, more attention must be paid to preventing current breakdown during sample collection. A ‘porous polymer joint’ sheathless interface for CE-MALDI off-line coupling was constructed by Wang et al. [77, 78]. A fracture was opened near the outlet end of CE separation capillary and was covered with cellulose acetate membrane allowing ions to go through for electric conduction. This porous polymer joint was immersed in buffer vial with grounded electrode, and the capillary column end went through the vial for sample deposition. The pressure-initiated capillary siphoning generated a low hydrodynamic flow (<100 nL/min), facilitating direct sample fraction deposition on Parafilm-coated MALDI target. CE separation of neuropeptides was driven in a reversed-polarity mode with acidic BGE. In conjunction with stable isotopic labelling, this off-line CE-MALDI-MS platform was further applied in the relative quantitation of crustacean peptidome in response to salinity stress [79].

Another sheathless interface introduced by the Girault group employs silver coated capillary column outlet for iontophoretic sample deposition on MALDI target (Figure 5) [80, 81]. Individual droplets of several microlitres were predeposited on the MALDI target to receive CE zones exiting the capillary end by electromigration and diffusion when the capillary tip dipped into these droplets. This approach allows using neutral capillary coating that eliminates EOF, and current breakdown during separation process could be avoided even without a sheath liquid flow or a bulk flow from inside of the capillary. The grounded capillary end was lifted from and dipped into a droplet at a relatively high frequency (~ 15 second per step), however, the electropherograms recorded by UV detector did not show a decrease in separation efficiency.

While most MALDI interfaces require mechanical motors to move the MALDI target to switch sample deposition position, Gorbatsova et al. used a digital microfluidic (DMF) board to manipulate the movement of collected droplets and send them to preset location [82]. In this setup, the positions of capillary column end and the microfluidic board were both fixed. Droplets of 3 μL volume, generated from a second 150 μm OD capillary tip positioned very close to the gold and silver coated separation column outlet, were responsible for maintaining electric continuity and carrying CE analytes onto a hydrophobic film covered DMF board. Operated based on the electrowetting on dielectric (EWOD) phenomenon, the DMF board with a set of 14 electrodes transported the collected droplets to different positions on the film. The film was lifted off the board and affixed to a MALDI target after solvent evaporation.

3.3 CE-MALDI-MSI

For off-line CE-MALDI-MS coupling, the time interval among sample depositions determines the efficiency of transferring the on-column peak resolution to the on-target peak resolution. Although higher resolution could be retained on MALDI target by using a faster sample deposition rate, loss of on-column resolution always occurs by collecting discrete fractions. Collecting continuous CE traces on a moving target followed by MALDI-MS detection along the whole trace could alleviate this problem. This concept was first attempted by van Veeleen et al. in 1993 using a sheath liquid interface [83], and actually

realized by Zhang et al. later employing a sheathless interface for depositing sample on a grounded s.s. target covered with cellulose membrane [84]. In that report, they used a 250 μm step size for acquiring mass spectra along the collected CE trace, which corresponded to 1 second online data sampling rate. The theoretical plate numbers of CE peaks from reconstructed electropherograms based on off-line MALDI detection were reported to be as high as 80−90% of those from on-line UV detection. With the development of MALDI-MSI hardware and software tools, nowadays it is possible to achieve step size as small as tens of microns on commercialized MALDI-ToF or MALDI-LTQ-Orbitrap instruments, which significantly improves the on-target electrophoretic peak resolution. Ideally, the on-column peak resolution could be fully retained by collecting continuous trace and using small enough raster step during imaging of collected trace. However, on-target sample dispersion during deposition and effluent sticking on the capillary outlet could also deteriorate the on-plate peak resolution and peak shape. Hence, it is preferable to use interfaces without coaxial sheath liquid for continuous trace collection in CE-MALDI-MSI applications.

In order to collect the continuous CE flow efficiently for the following MALDI-MS detection, Amantonico et al. used a customized MALDI target coated with omniphobic polysilazane nanocoating, which was also incorporated with an array of parallel grooves acting as recipients of the CE effluent [85]. Before separation, matrix dissolved in organic solvents was channeled into the 400 μm wide and 100 μm deep grooves and formed homogeneous coverage due to the modified surface wettability. During the CE run, the circuit at the outlet was completed by keeping the column end in contact with the grounded MALDI target. The capillary outlet was secured by a polytetrafluoroethylene (PTEE) sleeve, whose hydrophobicity helped preventing droplets attaching on the column end. The parallel grooves enabled multiplexing experiments by conducting CE separations in parallel columns simultaneously. Analysis of metabolites from yeast cell lysate in both positive and negative ionization mode was demonstrated on this platform.

Further improvements on coupling CE with MALDI-MSI were reported by Li and co-workers [86, 87]. They first used a pressurized liquid junction interface combined with grooved MALDI target plate for continuous trace deposition [86]. A capillary section with a fracture near the outlet was immersed in a pressurized liquid reservoir that was grounded through a platinum electrode. The pressure in the liquid reservoir combined with EOF created steady flow for sample deposition in the grooves with matrix pre-applied by air brush. The groove width was narrowed down to 250 μm to reduce on-target radial dispersion, and the distal end of the 360 OD capillary column was etched to 150 μm by hydrofluoric acid to fit the width of the groove. With the target moving at a speed of 110 μm/s during sample collection and 100 μm spatial resolution for MALDI-MSI detection, the reconstructed extracted ion electropherogram (Figure 6A) of several peptides showed similar separation efficiency as the UV detected electropherogram (Figure 6B). To avoid sample dilution introduced by the make-up flow from the liquid junction, another pressure assisted (PA) CE-MALDI-MSI interface (Figure 7A) [87] was constructed later based on the ‘porous polymer joint’ sheathless interface [77] developed earlier by the same group. Gravity induced hydrodynamic flow, as well as EOF contributed to the bulk flow in the separation column, which was mixed with the matrix flow delivered by another capillary at the tip and immediately deposited on a moving ground s. s. MALDI plate without grooving.

Capillary with smaller OD of 190 μm was used in this interface to minimize the sample dispersion on the target. Both CE-MALDI-MSI platforms were evaluated by relative quantification of peptide mixtures via isotopically labeled formaldehyde. Compared to CE-MALDI via discrete spot/fraction collection, improved peptidome coverage was achieved by CE-MALDI-MSI because of better preservation of separation efficiency on the MALDI target. 46 tryptic peptides from bovine serum albumin and 150 putative neuropeptides extracted from crustacean neural organs were observed with PACE-MSI (Figure 7B). Combined with reversed phase HPLC fractionation, this PACE-MSI platform demonstrated powerful separation efficiency in the analysis of orcokinin family neuropeptides from crude neural tissue extracts [88]. These innovations on CE-MALDI-MSI based techniques provide new approaches for the analysis of trace-level analytes from complex biological samples.

3.4 CIEF and GCE coupled with MALDI-MS

Off-line coupling of CIEF with MALDI-MS detection usually involves two steps: (1) isoelectric focusing, which could be performed with a conventional CE setup or a modified setup facilitating the subsequent sample collection; (2) mobilizing the focusing sample zones while depositing them on a MALDI sample plate. Different approaches to accomplish these two steps were adopted by researchers. If the conventional CE apparatus is used for focusing, the voltage has to be stopped to remove the catholyte vial, and the capillary outlet could be directly used for sample deposition on a MALDI target [89, 90] or directed to a coaxial sheath liquid deposition device [91]. A more convenient way would be using the same setup for both CIEF focusing and mobilization/sample deposition. Lechner et al. used a spotting robot, which actually worked as a grounded coaxial sheath liquid interface, for electric connection and catholyte supply during the focusing and pressure mobilization process [92]. The catholyte sheath liquid helped creating droplets and the matrix was deposited by another capillary. The ‘porous polymer joint’, previously employed for pressure assisted CZE-MALDI-MS coupling [77], was also adopted by Cheng et al. in CIEF-MALDI-MS application [93]. Electrophoretic mobilization could be an option, but extra procedures would be involved to switch the catholyte solution to mobilizer solution at the beginning of mobilization. Therefore, most researchers still prefer to adopt pressure mobilization with voltage applied across the capillary during sample collection. In spite of technical challenges with the instrumentation, CIEF-MALDI-MS applications in examining the microheterogeneity of intact glycoproteins [94], discovering novel neuropeptides [89], characterizing glycopeptides and phosphopeptides [92] were demonstrated by several groups.

A major issue for CIEF-MALDI-MS coupling is the suppressed ionization efficiency caused by high concentration of carrier ampholytes, viscosity-increasing agents, and protein solubilising detergents. Systematical evaluation of MALDI signal suppression caused by these additives was performed by Silverland et al., and it was concluded that compromises have to be made between the separation efficiency and repeatability on one hand and MS signal intensity on the other [95]. Cheng et al. reported a special sample deposition method to alleviate the protein signal suppression [93]. A rough on-target separation of proteins and additives was achieved by depositing 0.1 μL of CIEF fraction into a 1 μL water droplet on a MALDI plate. While the smaller additive molecules (carrier ampholytes, detergents, and

salts) diffused faster toward the edge of water droplet, most protein molecules remained at the centre region. After solvent evaporation, 0.5 μL of matrix solution was added for co-crystallization. 2–10 fold of S/N ratio improvement in protein signals was reported; however, it may still suffer from limitations for analysis of smaller peptides due to similar molecular weight range as the carrier ampholytes. Another potential solution to this problem, coupling monolithic column based immobilized pH-gradient CIEF with MALDI-MS, was proposed and demonstrated by Zhang et al. [96]. Instead of mixing with sample prior to focusing, carrier ampholytes were loaded into the separation capillary, pre-focused and linked to the epoxy groups on the monolith surface so that the pH gradient was immobilized. Enhanced MALDI MS signal intensities were observed due to the elimination of carrier ampholytes from sample. Choice of monolith fabrication material might be further optimized for avoiding hydrophobic interaction between monolith surface and peptides and proteins while retaining the rigidity of the monolith.

An additional advantage of off-line coupling is that post-separation sample treatment can be performed if necessary. A good example was demonstrated by coupling SDS-CGE and MALDI-TOFMS for protein separation and characterization [97]. A strip of poly(tetrafluoroethylene) (PTEF) membrane immersed in outlet buffer reservoir was used to collect the CGE separated SDS-protein complexes. After sample collection, the membrane was washed with 0.40% Tergitol NP Type 40 at 40 °C for 60 minutes to remove the SDS bound to proteins. Then the PTEF membrane with SDS-free proteins was attached to MALDI target for MS detection.

3.5 Microfluidic device based CE-MALDI MS

Coupling microfluidic device-based CE to MALDI-MS is still facing difficulties, such as collecting the narrow peaks on chip, transferring the collected fraction from a microfluidic chip to a MALDI target efficiently. Only a limited number of reports described development in this area. A polydimethylsiloxane (PDMS) based microfluidic device, reported by Luo et al., was applied to on-chip CE separation and fractionation followed by MALDI-MS detection [98]. Instead of collecting sample zones at the capillary outlet end during an on-going run, the separated sample zones distributing along the separation channel were segmented and collected for MALDI-MS. After a brief voltage application, the separation was stopped and valves along the separation channels were closed to form segmented compartments. By actuating the pumps in the control layer, these in-channel fractionated sample segments were sent to individual micro reservoirs by pressure via a series of branched channels connected to the separation channel. Then the collected microliter volume fractions were transferred out of the microfluidic device by dispensing tools for the subsequent MALDI-MS detection. The separation resolution was significantly limited by the number of fractions that could be collected on the chip; and the detection sensitivity could also be compromised by the sample loss during transferring the microliter fractions from the microfluidic device to the MALDI target.

4 Concluding remarks

This review summarizes recent technological advances in the development and application of interfacing CE based separation techniques with ESI and MALDI MS detection for biomolecule analysis. While LC-ESI-MS remains the most widely used platform for 'omics' research, growing interests in the application of CE-ESI-MS in the analysis of small molecules, peptides as well as proteins have been propelled by the evolving and ever-improving interface designs. Improvements on interface robustness, ionization efficiency, signal stability and reproducibility make CE-ESI-MS a complementary or an even superior tool in specific applications, especially in the analyses of small hydrophilic metabolites, short peptides and post-translational modification of proteins. Although MALDI-MS is seldom used for label-free quantification, CE-MALDI-MS integrated with isotopic labeling [79, 86, 87] or iTRAQ labeling [99] has proven to be effective in multiplexed relative quantification of peptides or protein digests from complex biological samples. High spatial resolution of MALDI-MS imaging (MSI) enables almost complete retention of the on-column separation efficiency. The reconstructed electropherograms of isotopically labeled peptide pairs allow for quantitative analysis, making CE-MALDI-MSI a promising technique for samples that could not be well resolved or efficiently ionized by on-line CE-ESI-MS. With the fast development in CE-MS instrumentation, we envision that this analytical platform would find greater utility for many routine analyses in analytical laboratories and provide powerful tools to solve challenging biological problems.

Acknowledgments

Preparation of this manuscript was supported in part by National Science Foundation (CHE- 0957784) and National Institutes of Health through grant 1R01DK071801. L.L. acknowledges an H. I. Romnes Faculty Fellowship.

References

1. Ramautar R, Somsen GW, de Jong GJ. Electrophoresis. 2013; 34:86–98. [PubMed: 23161106]
2. Kuehnbaum NL, Britz-McKibbin P. Chem. Rev. 2013; 113:2437–2468. [PubMed: 23506082]
3. Zhao SS, Zhong XF, Tie C, Chen DDY. Proteomics. 2012; 12:2991–3012. [PubMed: 22888086]
4. Krenkova J, Foret F. Proteomics. 2012; 12:2978–2990. [PubMed: 22888067]
5. Ramautar R, Heemskerk AAM, Hensbergen PJ, Deelder AM, Busnel JM, Mayboroda OA. J. Proteomics. 2012; 75:3814–3828. [PubMed: 22609513]
6. Fonslow BR, Yates JR. J. Sep. Sci. 2009; 32:1175–1188. [PubMed: 19360788]
7. Desiderio C, Rossetti DV, Iavarone F, Messana I, Castagnola M. J. Pharm. Biomed. Anal. 2010; 53:1161–1169. [PubMed: 20674216]
8. Mechref Y, Novotny MV. Mass Spectrom. Rev. 2009; 28:207–222. [PubMed: 18973241]
9. Haselberg R, de Jong GJ, Somsen GW. Electrophoresis. 2013; 34:99–112. [PubMed: 23161520]
10. Hommerson P, Khan AM, de Jong GJ, Somsen GW. Mass Spectrom. Rev. 2011; 30:1096–1120. [PubMed: 21462232]
11. Zamfir AD. J. Chromatogr. A. 2007; 1159:2–13. [PubMed: 17428492]
12. Maxwell EJ, Chen DDY. Anal. Chim. Acta. 2008; 627:25–33. [PubMed: 18790125]
13. Klampfl CW. Electrophoresis. 2009; 30:S83–S91. [PubMed: 19517505]
14. Bonvin G, Schappler J, Rudaz S. J. Chromatogr. A. 2012; 1267:17–31. [PubMed: 22846629]
15. Smith RD, Barinaga CJ, Udseth HR. Anal. Chem. 1988; 60:1948–1952.
16. Lapainis T, Rubakhin SS, Sweedler JV. Anal. Chem. 2009; 81:5858–5864. [PubMed: 19518091]

17. Nemes P, Knolhoff AM, Rubakhin SS, Sweedler JV. Anal.Chem. 2011; 83:6810–6817. [PubMed: 21809850]
18. Nemes P, Rubakhin SS, Aerts JT, Sweedler JV. Nat. Protoc. 2013; 8:783–799. [PubMed: 23538882]
19. Nemes P, Knolhoff AM, Rubakhin SS, Sweedler JV. ACS Chem. Neurosci. 2012; 3:782–792. [PubMed: 23077722]
20. Knolhoff AM, Nautiyal KM, Nemes P, Kalachikov S, Morozova I, Silver R, Sweedler JV. Anal. Chem. 2013; 85:3136–3143. [PubMed: 23409944]
21. Fanali S, D'Orazio G, Foret F, Kleparnik K, Aturki Z. Electrophoresis. 2006; 27:4666–4673. [PubMed: 17091468]
22. Kusy P, Kleparnik K, Aturki Z, Fanali S, Foret F. Electrophoresis. 2007; 28:1964–1969. [PubMed: 17486659]
23. D'Orazio G, Fanali S. J. Chromatogr. A. 2010; 1217:4079–4086. [PubMed: 19945112]
24. Tomas R, Koval M, Foret F. J. Chromatogr. A. 2010; 1217:4144–4149. [PubMed: 20219201]
25. Hezinova V, Aturki Z, Kleparnik K, D'Orazio G, Foret F, Fanali S. Electrophoresis. 2012; 33:653–660. [PubMed: 22451058]
26. Kleparnik K, Otevrel M. Electrophoresis. 2010; 31:879–885. [PubMed: 20191549]
27. Maxwell EJ, Zhong XF, Zhang H, van Zeijl N, Chen DDY. Electrophoresis. 2010; 31:1130–1137. [PubMed: 20196027]
28. Wojcik R, Dada OO, Sadilek M, Dovichi NJ. Rapid Commun. Mass Spectrom. 2010; 24:2554–2560. [PubMed: 20740530]
29. Maxwell EJ, Zhong XF, Chen DDY. Anal. Chem. 2010; 82:8377–8381. [PubMed: 20873780]
30. Zhu G, Sun L, Wojcik R, Kernaghan D, McGivney JB, Dovichi NJ. Talanta. 2012; 98:253–256. [PubMed: 22939156]
31. Sun L, Li Y, Champion MM, Zhu G, Wojcik R, Dovichi NJ. Analyst. 2013; 138:3181–3188. [PubMed: 23591184]
32. Li Y, Champion MM, Sun L, Champion PAD, Wojcik R, Dovichi NJ. Anal.Chem. 2012; 84:1617–1622. [PubMed: 22182061]
33. Sun LL, Zhu GJ, Li YH, Wojcik R, Yang P, Dovichi NJ. Proteomics. 2012; 12:3013–3019. [PubMed: 22888077]
34. Wojcik R, Li Y, MacCoss MJ, Dovichi NJ. Talanta. 2012; 88:324–329. [PubMed: 22265506]
35. Zhu G, Sun L, Yang P, Dovichi NJ. Anal. Chim. Acta. 2012; 750:207–211. [PubMed: 23062442]
36. Sun LL, Zhu GJ, Dovichi NJ. Anal. Chem. 2013; 85:4187–4194. [PubMed: 23510126]
37. Zhu G, Sun L, Yan X, Dovichi NJ. Anal. Chem. 2013; 85:2569–2573. [PubMed: 23394296]
38. Zhong XF, Maxwell EJ, Chen DDY. Anal. Chem. 2011; 83:4916–4923. [PubMed: 21528898]
39. Maxwell EJ, Ratnayake C, Jayo R, Zhong XF, Chen DDY. Electrophoresis. 2011; 32:2161–2166. [PubMed: 21792989]
40. Jayo RG, Li JJ, Chen DDY. Anal. Chem. 2012; 84:8756–8762. [PubMed: 22971167]
41. Zhong XF, Maxwell EJ, Ratnayake C, Mack S, Chen DDY. Anal. Chem. 2011; 83:8748–8755. [PubMed: 21972844]
42. Moini M. Anal. Chem. 2007; 79:4241–4246. [PubMed: 17447730]
43. Faserl K, Sarg B, Kremser L, Lindner H. Anal. Chem. 2011; 83:7297–7305. [PubMed: 21848273]
44. Tie C, Zhang DW, Chen HX, Song SL, Zhang XX. J. Mass Spectrom. 2012; 47:1429–1434. [PubMed: 23147818]
45. Busnel JM, Schoenmaker B, Ramautar R, Carrasco-Pancorbo A, Ratnayake C, Feitelson JS, Chapman JD, Deelder AM, Mayboroda OA. Anal. Chem. 2010; 82:9476–9483. [PubMed: 21028888]
46. Heemskerk AAM, Busnel JM, Schoenmaker B, Derks RJE, Klychnikov O, Hensbergen PJ, Deelder AM, Mayboroda OA. Anal. Chem. 2012; 84:4552–4559. [PubMed: 22494114]
47. Heemskerk AAM, Wuhrer M, Busnel JM, Koeleman CAM, Selman MHJ, Vidarsson G, Kapur R, Schoenmaker B, Derks RJE, Deelder AM, Mayboroda OA. Electrophoresis. 2013; 34:383–387. [PubMed: 23161657]

48. Haselberg R, de Jong GJ, Somsen GW. Anal. Chem. 2013; 85:2289–2296. [PubMed: 23323765]
49. Bonvin G, Veuthey JL, Rudaz S, Schappler J. Electrophoresis. 2012; 33:552–562. [PubMed: 22451047]
50. Hirayama A, Tomita M, Soga T. Analyst. 2012; 137:5026–5033. [PubMed: 23000847]
51. Ramautar R, Busnel JM, Deelder AM, Mayboroda OA. Anal. Chem. 2012; 84:885–892. [PubMed: 22148170]
52. Whitmore CD, Gennaro LA. Electrophoresis. 2012; 33:1550–1556. [PubMed: 22736356]
53. Haselberg R, Ratnayake CK, de Jong GJ, Somsen GW. J. Chromatogr. A. 2010; 1217:7605–7611. [PubMed: 20970804]
54. Nguyen A, Moini M. Anal. Chem. 2008; 80:7169–7173. [PubMed: 18710259]
55. Moini M. Rapid Commun. Mass Spectrom. 2010; 24:2730–2734. [PubMed: 20814979]
56. Haselberg R, Harmsen S, Dolman MEM, de Jong GJ, Kok RJ, Somsen GW. Anal.Chim. Acta. 2011; 698:77–83. [PubMed: 21645662]
57. Moini M, Klauenberg K, Ballard M. Anal. Chem. 2011; 83:7577–7581. [PubMed: 21913691]
58. Kawai M, Iwamuro Y, Iio-Ishimaru R, Chinaka S, Takayama N, Hayakawa K. Anal. Sci. 2011; 27:857–860. [PubMed: 21828926]
59. Ramautar R, Shyti R, Schoenmaker B, de Groote L, Derks RJE, Ferrari MD, van den Maagdenberg A, Deelder AM, Mayboroda OA. Anal. Bioanal. Chem. 2012; 404:2895–2900. [PubMed: 23052875]
60. Wang Y, Fonslow BR, Wong CCL, Nakorchevsky A, Yates JR. Anal. Chem. 2012; 84:8505–8513. [PubMed: 23004022]
61. Sarg B, Faserl K, Kremser L, Halfinger B, Sebastiano R, Lindner HH. Mol. Cell Proteomics. 2013; 12:2640–2656. [PubMed: 23720761]
62. Shi LH, Jin YX, Moon DC, Kim SK, Park SR. Electrophoresis. 2009; 30:1661–1669. [PubMed: 19343727]
63. Jeong JS, Kim SK, Park SR. Electrophoresis. 2012; 33:2112–2121. [PubMed: 22821486]
64. Huang JL, Hsu RY, Her GR. J. Chromatogr. A. 2012; 1267:131–137. [PubMed: 22975356]
65. Li FA, Wang CH, Her GR. Electrophoresis. 2007; 28:1265–1273. [PubMed: 17366484]
66. Li FA, Huang JL, Her GR. Electrophoresis. 2008; 29:4938–4943. [PubMed: 19130573]
67. Hoffmann P, Hausig U, Schulze P, Belder D. Angew. Chem.-Int. Edit. 2007; 46:4913–4916.
68. Hoffmann P, Eschner M, Fritzsche S, Belder D. Anal. Chem. 2009; 81:7256–7261. [PubMed: 19639956]
69. Fritzsche S, Hoffmann P, Belder D. Lab Chip. 2010; 10:1227–1230. [PubMed: 20445873]
70. Mellors JS, Gorbounov V, Ramsey RS, Ramsey JM. Anal. Chem. 2008; 80:6881–6887. [PubMed: 18698800]
71. Mellors JS, Jorabchi K, Smith LM, Ramsey JM. Anal. Chem. 2010; 82:967–973. [PubMed: 20058879]
72. Chambers AG, Mellors JS, Henley WH, Ramsey JM. Anal. Chem. 2011; 83:842–849. [PubMed: 21214194]
73. Mellors JS, Black WA, Chambers AG, Starkey JA, Lacher NA, Ramsey JM. Anal. Chem. 2013; 85:4100–4106. [PubMed: 23477683]
74. Huck CW, Bakry R, Huber LA, Bonn GK. Electrophoresis. 2006; 27:2063–2074. [PubMed: 16645982]
75. Helmja K, Borissova M, Knjazeva T, Jaanus M, Muinasmaa U, Kaljurand M, Vaher M. J. Chromatogr. A. 2009; 1216:3666–3673. [PubMed: 19147148]
76. Vannatta MW, Whitmore CD, Dovichi NJ. Electrophoresis. 2009; 30:4071–4074. [PubMed: 19960472]
77. Wang J, Ma M, Chen R, Li L. Anal. Chem. 2008; 80:6168–6177. [PubMed: 18642879]
78. Wang JH, Jiang XY, Sturm RM, Li LJ. J. Chromatogr. A. 2009; 1216:8283–8288. [PubMed: 19473662]
79. Wang J, Zhang Y, Xiang F, Zhang Z, Li L. J. Chromatogr. A. 2010; 1217:4463–4470. [PubMed: 20334868]

80. Pourhaghighi MR, Busnel JM, Girault HH. Electrophoresis. 2011; 32:1795–1803. [PubMed: 21710548]
81. Busnel JM, Josserand J, Lion N, Girault HH. Anal. Chem. 2009; 81:3867–3872. [PubMed: 19374373]
82. Gorbatsova J, Borissova M, Kaljurand M. Electrophoresis. 2012; 33:2682–2688. [PubMed: 22965712]
83. Vanveelen PA, Tjaden UR, Vandergreef J, Ingendoh A, Hillenkamp F. J. Chromatogr. 1993; 647:367–374.
84. Zhang HY, Caprioli RM. J. Mass Spectrom. 1996; 31:1039–1046. [PubMed: 8831154]
85. Amantonico A, Urban PL, Zenobi R. Analyst. 2009; 134:1536–1540. [PubMed: 20448916]
86. Wang JH, Ye H, Zhang ZC, Xiang F, Girdaukas G, Li LJ. Anal. Chem. 2011; 83:3462–3469. [PubMed: 21417482]
87. Zhang ZC, Ye H, Wang JH, Hui LM, Li LJ. Anal. Chem. 2012; 84:7684–7691. [PubMed: 22891936]
88. Zhang ZC, Jia CX, Li LJ. J. Sep. Sci. 2012; 35:1779–1784. [PubMed: 22807360]
89. Hui LM, Cunningham R, Zhang ZC, Cao WF, Jia CX, Li LJ. J. Proteome Res. 2011; 10:4219–4229. [PubMed: 21740068]
90. Zhang ZC, Wang JH, Hui LM, Li LJ. J. Chromatogr.A. 2011; 1218:5336–5343. [PubMed: 21696746]
91. Weiss NG, Zwick NL, Hayes MA. J.Chromatogr. A. 2010; 1217:179–182. [PubMed: 19945710]
92. Lechner M, Seifner A, Rizzi AM. Electrophoresis. 2008; 29:1974–1984. [PubMed: 18425755]
93. Cheng CA, Lu JAJ, Wang XY, Roberts J, Liu SR. Electrophoresis. 2010; 31:2614–2621. [PubMed: 20603827]
94. Weiss NG, Jarvis JW, Nelson RW, Hayes MA. Proteomics. 2011; 11:106–113. [PubMed: 21182198]
95. Silvertand LHH, Torano JS, de Jong GJ, van Bennekom WP. Electrophoresis. 2009; 30:1828–1835. [PubMed: 19391148]
96. Zhang ZC, Wang JH, Hui LM, Li LJ. Electrophoresis. 2012; 33:661–665. [PubMed: 22451059]
97. Lu JJ, Zhu ZF, Wang W, Liu SR. Anal. Chem. 2011; 83:1784–1790. [PubMed: 21309548]
98. Luo YQ, Xu SY, Schilling JW, Lau KH, Whitin JC, Yu TTS, Cohen HJ. Jala. 2009; 14:252–261.
99. Zuberovic A, Wetterhall M, Hanrieder J, Bergquist J. Electrophoresis. 2009; 30:1836–1843. [PubMed: 19441030]

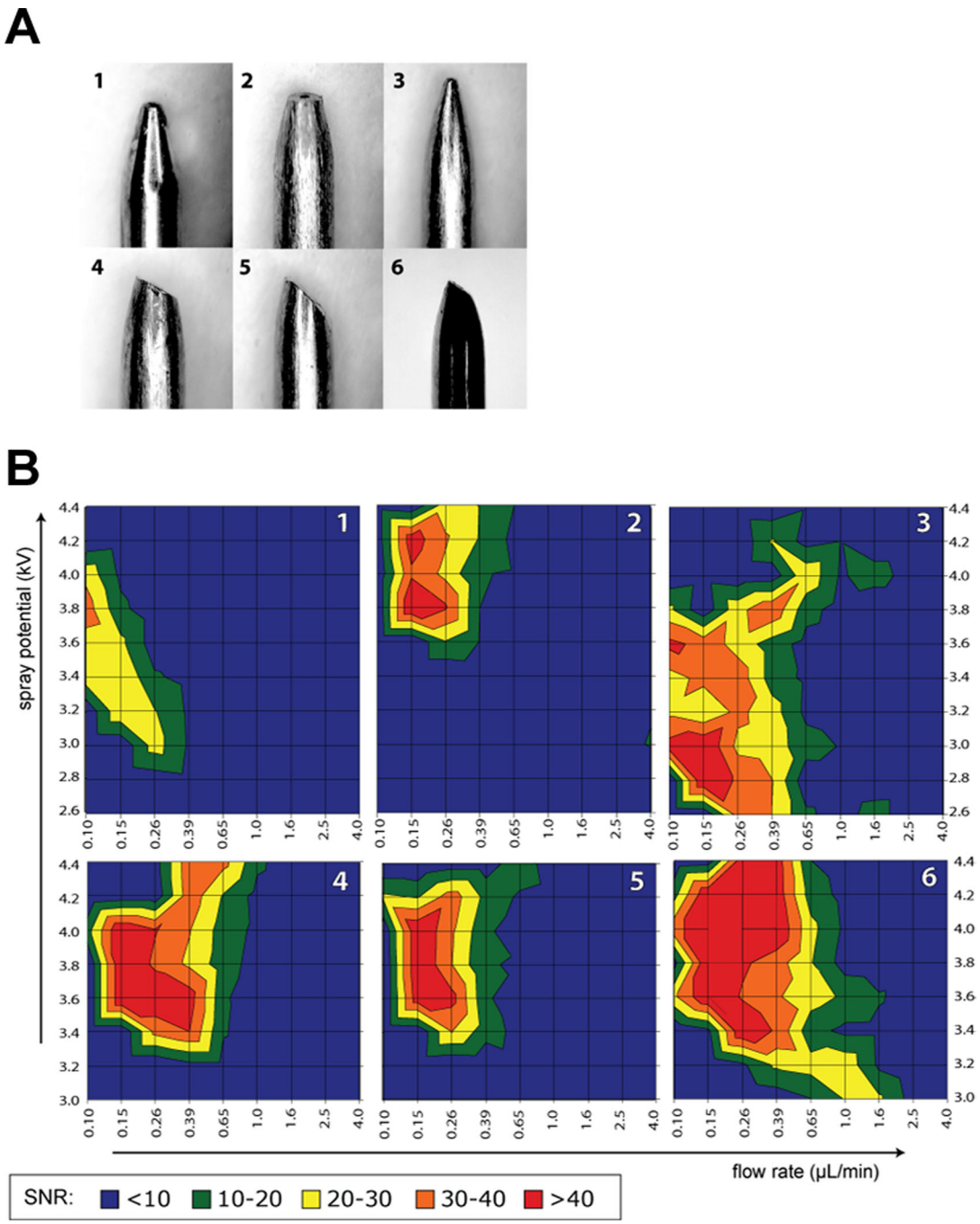

Figure 1.

(A) Different shapes of stainless steel electrospray emitters investigated for optimal ESI performance: symmetrically tapered electrospray needle (**1**), blunt tapered tip (**2**), sharp tapered needle (**3**), 30° bevel tip made from **2** (**4**), 45° bevel tip made from **2** (**5**), 35° bevel tip with a smaller surface area (**6**). (B) Average signal-to-noise ratio of arginine as a function of flow rate and electrospray potential. Emitter geometry for each plot is indicated in the top right corner. Sample: 20 μM each of proline, threonine, isoleucine, and arginine in 0.2% formic acid and 50% methanol. Reprinted with permission from Ref [29]. Copyright American Chemical Society 2010.

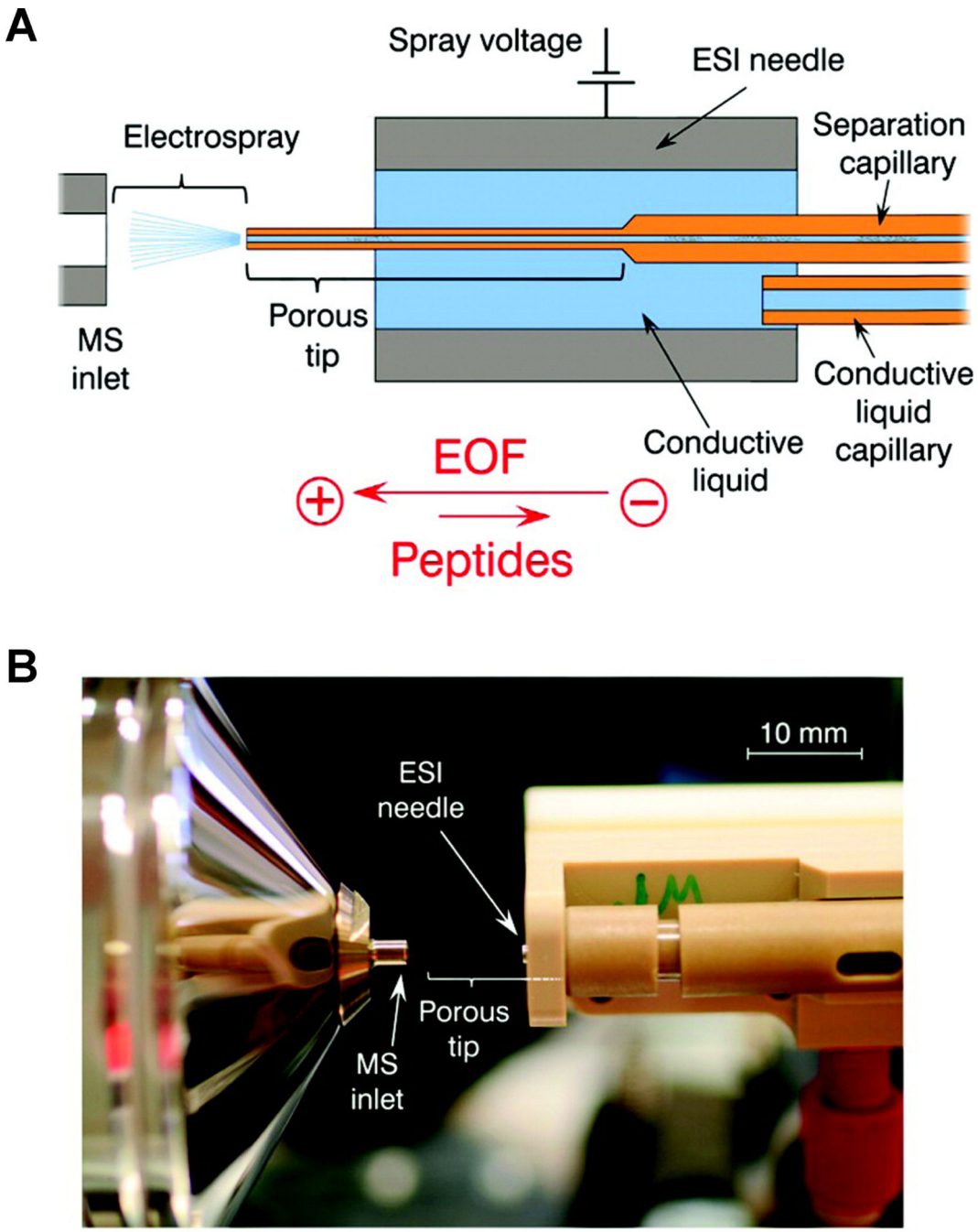

Figure 2.

The high-sensitivity porous sprayer interface (A) schematic and (B) photograph of the prototype interface. Reprinted with permission from Ref [43]. Copyright American Chemical Society 2011.

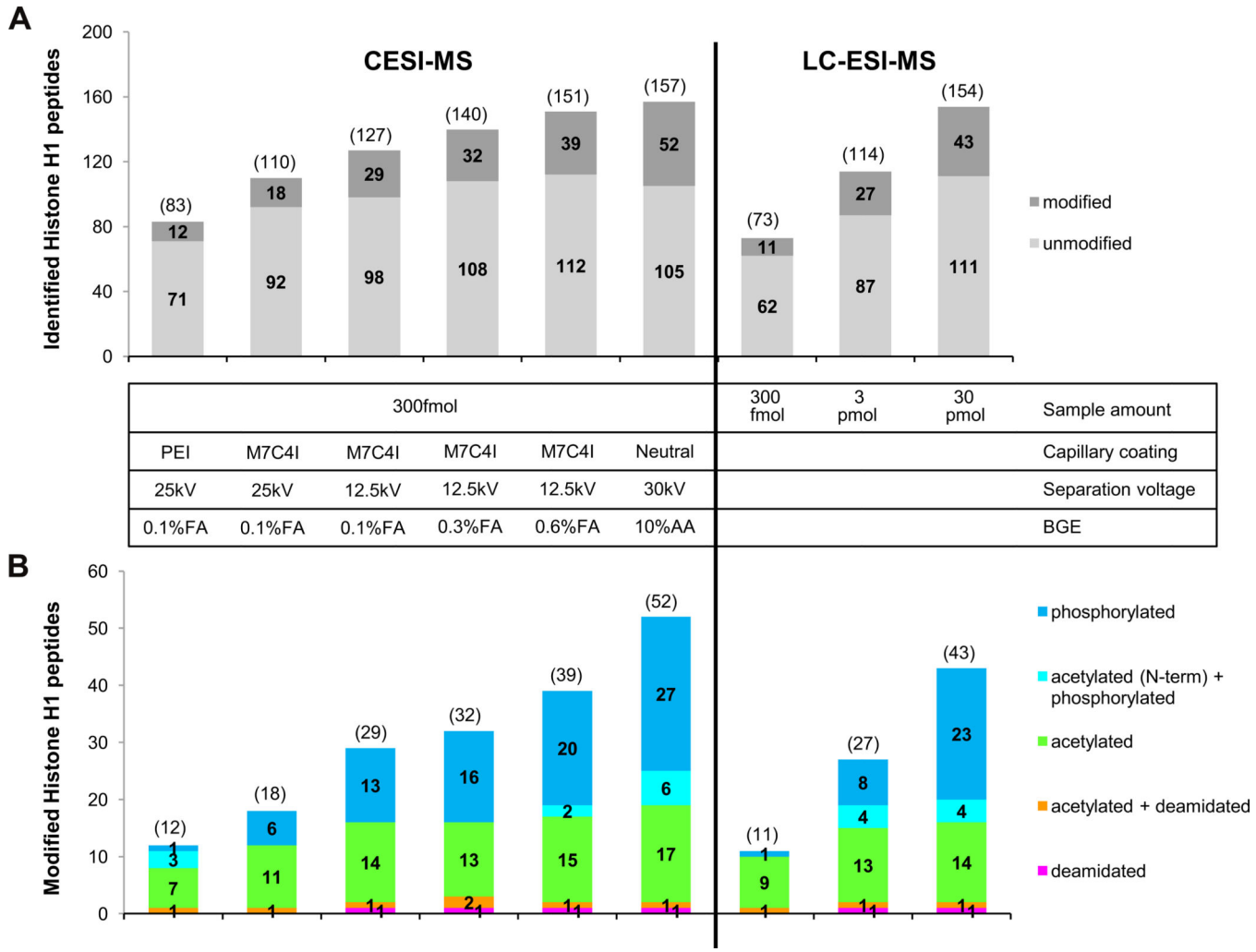

Figure 3.

Number of unmodified and modified histone H1 peptides identified by CE- and LC-ESI-MS/MS analysis. (A) Number of identified histone H1 peptides (modified and non-modified) were merged from triplicate analyses. (B) Within each column the total number of modified peptides as well as the distribution of specific types of modifications is shown. The numbers presented in the diagram are the sum of unique modified peptides found in triplicate runs. Overlap of peptides identified with CE-ESI-MS ranges from 75% – 84%, with LC-ESI-MS from 66% – 71%. Reprinted with permission from Ref [61]. Copyright American Society for Biochemistry and Molecular Biology 2013.

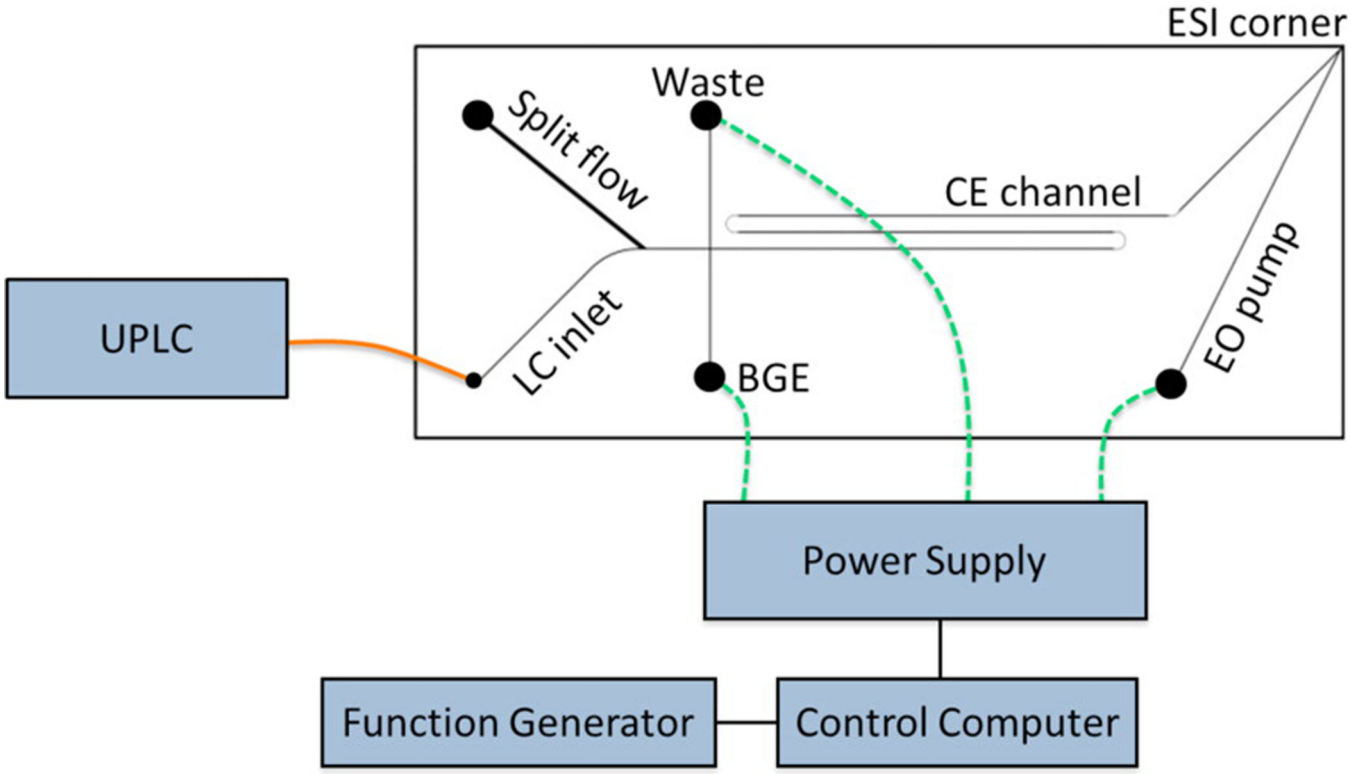

Figure 4.

Schematic of the hybrid capillary LC microchip CE-ESI experimental setup. The orange line represents a transfer capillary connecting the LC column to the microfluidic device. The dashed green lines represent electrical connections between the high voltage power supply and the microfluidic reservoirs. The device was positioned with the ESI corner approximately 5 mm from the mass spectrometer inlet. Reprinted with permission from Ref [73]. Copyright American Chemical Society 2013.

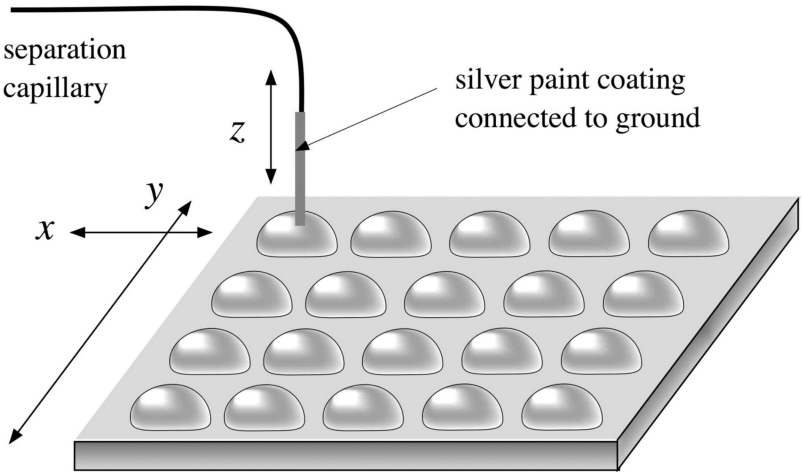

Figure 5.

CE-MALDI-MS interface by iontophoretic fraction collection. A separation capillary silver-coated at the tip was dipped into droplets predeposited on the MALDI plate mounted on an x-y stage. Fractions were collected based on electro-migration and diffusion. Reprinted with permission from Ref [81] Copyright American Chemical Society 2009.

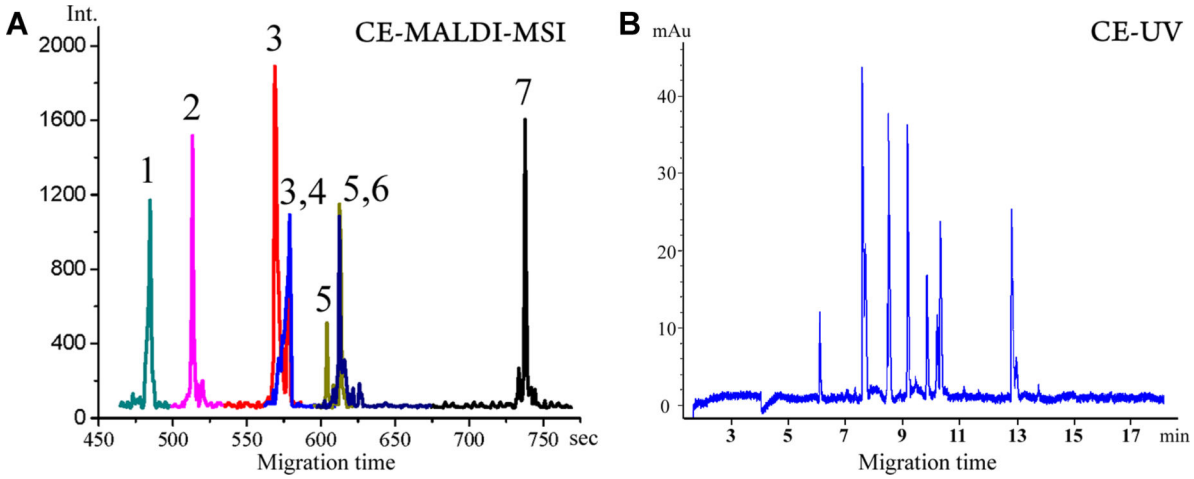

Figure 6.

(A) Reconstructed CE electropherogram from MALDI TOF/TOF-MSI of seven peptide standards. The peak IDs are (1) GAHKNYLRF, *m/z* 1105.59 (0.70 μM), (2) IARRHPYFL, *m/z* 1172.67 (0.75 μM), (3) SGGFAFSPRLamide, *m/z* 1037.55 (0.65 μM), (4) CYFQNCPRGamide, *m/z* 1084.45 (0.37 μM), (5) APSGAQRLYGFGLamide, *m/z* 1335.72 (0.25 μM), (6) AGCKNFFWKTFTSC, *m/z* 1637.72 (0.55 μM), (7) PFCNAFTGCamide, *m/z* 956.37 (0.5 μM). (B) CE-UV electropherogram. Reprinted with permission from Ref [86] Copyright American Chemical Society 2011.

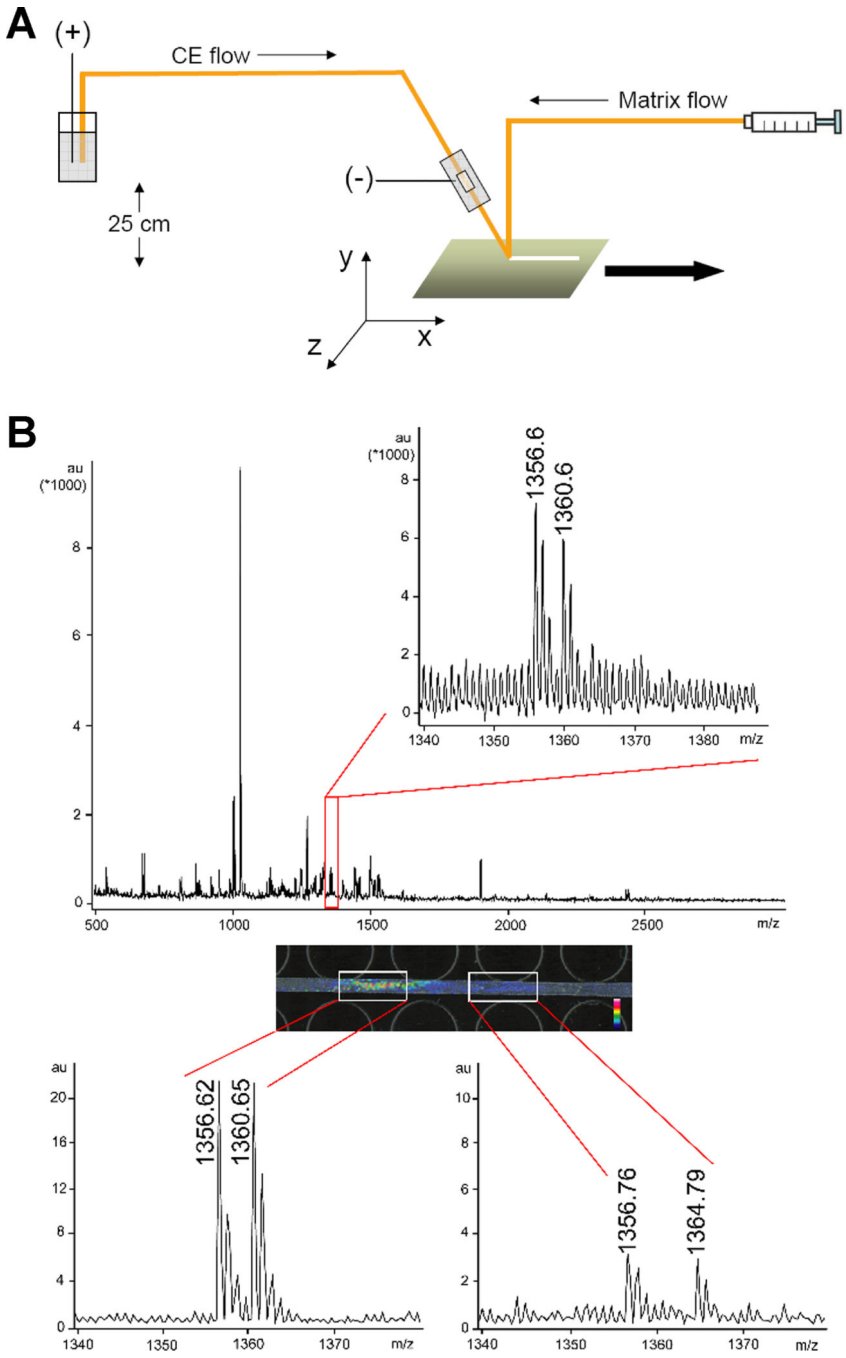

Figure 7.

Interface for pressure assisted CE-MALDI-MSI coupling. (A) CE flow and matrix flow are collected on a ground stainless steel MALDI plate. (B) Image-based analysis of isotopic labeled peptide peak pairs (1:1 concentration ratio) showing enhanced signal-to-noise ratios and improved quantitation accuracy. Reprinted with permission from Ref [87]. Copyright American Chemical Society 2012.